Journal of Magnetism and Magnetic Materials 36 (1983) 66–72
North-Holland Publishing Company

MAGNETIC RELAXATION MEASUREMENTS IN FeCr ALLOYS

A.C. PALUMBO

Department of Physics, University of Rochester, Rochester, NY 14627, USA

R.D. PARKS

Department of Physics, Polytechnic Institute of New York, Brooklyn, NY 11201, USA

and Y. YESHURUN

Department of Physics, Bar-Ilan University, Ramat-Gan 52100, Israel

Received 8 July 1982; in revised form 15 September 1982

Detailed magnetic measurements are presented for Fe_xCr_{1-x}, $0.12 \leqslant x \leqslant 0.24$. We focus on irreversible phenomena and present magnetic viscosity measurements for external magnetic fields 100 Oe $\leqslant H \leqslant 3$ kOe, in the temperature range 1.5 K $\leqslant T \leqslant$ 7.5 K. We find the border lines of the spin-glass phase via the disappearance of irreversible relaxation and construct a magnetic phase diaram for FeCr in the $H-T-x$ space.

1. Introduction

The spin glass is defined as a system of randomly oriented "frozen" spins with a non-zero time averaged magnitude for each spin but with no long-range magnetic order. In the infinite time limit this definition corrrsponds to the Edwards–Anderson (EA) spin-glass phase [1]. The solvable infinite range model proposed by Sherrington and Kirkpatrick [2] (SK) for the EA order parameter introduces a magnetic phase diagram containing paramagnetic (PM), ferromagnetic (FM) and spin-glass (SG) phases. One of the interesting predictions of this solution is the possibility of a temperature-driven FM → SG phase transition. Many experimental demonstrations of such a transition are known (see e.g., refs. [3]). Much less experimental work, however, has been devoted to the study of antiferromagnetic (AFM) → SG transitions [4] which were predicted theoretically in some short-range models of the EA order parameter [5]. The phase diagram in these models contain transitions from the PM state to the magnetic ordered (FM, AFM or SG) states as well as FM → SG and AFM → SG transitions. A realization of this complicated phase diagram seems to be the Fe_xCr_{1-x} system. It was demonstrated recently [3] that for $0.18 \lesssim x \lesssim 0.25$ the FM ordering fades at low temperature. Other experiments [6–8] show that for $0.10 \lesssim x \lesssim 0.15$ the AFM order vanishes at some low temperatures. In both cases, as well as for intermediate concentrations, many spin-glass-like phenomena are observed at low temperature. In particular, irreversible response phenomena, which are fingerprints of spin-glass systems, are found in FeCr at low temperature, but have not been studied systematically. In this article we explore the low temperature phase, which we refer to as a spin glass, in a series of FeCr samples. We focus on magnetic viscosity measurements and study the rate of relaxation as a function of temperature, field and iron concentration. Our goal is to construct an $H-T$ (field temperature) phase diagram for each FeCr alloy. This goal is motivated by recent theoretical developments [9–11] which predict field-induced SG/PM transitions. The so-called de Almeida–Thouless (AT) line is the borderline between the two phases. The transi-

0304-8853/83/0000–0000/$03.00

tions from the SG phase to the PM phase is detected via vanishing of relaxation phenomena [12]. Magnetic relaxation is therefore the appropriate probe for identification of the AT line. Several authors [13–16] have already tried this approach but the present article introduces the first study of the AT line in a number of concentrations ranging from the FM side to the AFM side of the phase diagram. We also use the same approach to demonstrate the SG borders on the concentration (x) axis. We conclude with an H–T–x phase diagram for FeCr.

2. Experimental

Polycrystalline boules of Fe_xCr_{1-x} samples ($x = 0.12$, 0.16, 0.17, 0.20, 0.22 and 0.24) were prepared from 99.99% starting materials which were arc melted, annealed for four days at 100°C, water quenched and then reannealed at 1000°C for another day to remove strains. Most of the samples were spheres with a radius of ≈ 0.4 cm. For $x = 0.22$ and 0.24 we also prepared needle-shaped samples. In the following sections we refer to results which were obtained for spherical samples unless it is explicitly stated otherwise. Corrections for demagnetization effects have been made wherever results for spheres and needles are compared.

A Faraday balance was used for all dc, irreversible phenomena measurements.

3. Results and discussion

We start this section with comparative magnetization results for $x = 0.12$ and $x = 0.22$. These samples represent materials from the AFM and the FM side respectively. In fig. 1 we show the dc magnetic susceptibility for $x = 0.22$ sample. The Curie temperature is [3] around 110 K. The circles describe the magnetization measured in 10 Oe after a zero field cooling (ZFC) process to 1.5 K. The squares describe the magnetization in a 10 Oe cooling field. The branch point at $T_B \approx 20$ K marks the appearance of irreversible phenomena. This temperature is pushed to lower values as the external field is increased. The plateau which is observed at intermediate temperature is due to demagnetization effects. The drop in this constant value is typical of re-entrant materials near the FM → SG transition temperature.

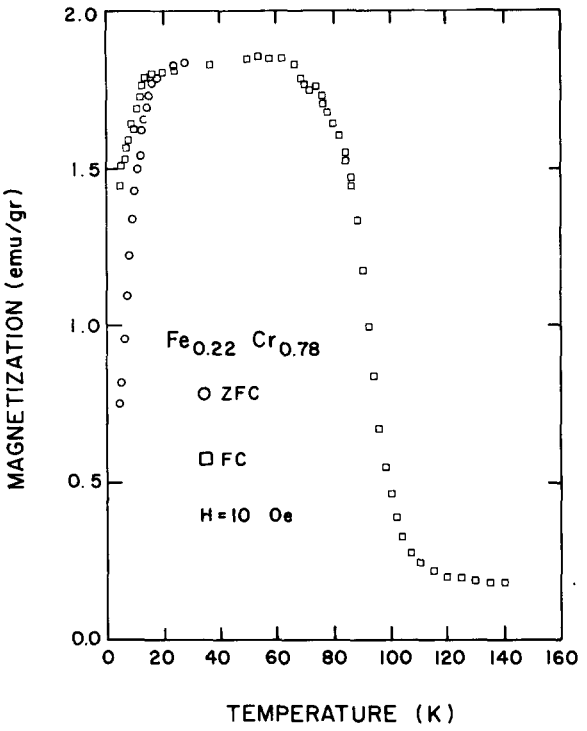

Fig. 1. Temperature dependence of the magnetic susceptibility in $Fe_{0.22}Cr_{0.78}$ measured in a 10 Oe magnetic field. Circles describe a zero field cooling process. Squares describe a field cooling process.

In fig. 2 we exhibit the magnetization of the AFM sample ($x = 0.12$). The circles and squares have the same meaning as in fig. 1. Also here the branch point depends on the magnitude of the measuring field. The arrow marks the PM → AFM transition as found in neutron diffraction experiments [6]. No sign for this transition is found via magnetization measurements. Note, however, the sharp peak at $T \approx 12.5$ K which suggests an AFM → SG transition.

The branch points which appear in figs. 1 and 2 occur at temperature $T_c(H)$ above which the zero field and the field-cooled susceptibilities coincide. Magnetic viscosity is observed below this tempera-

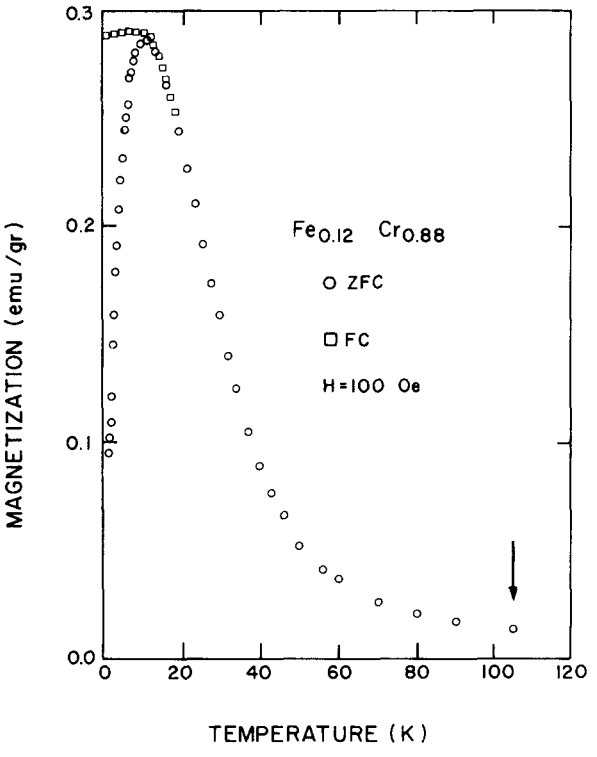

Fig. 2. Temperature dependence of the magnetic susceptibility in $Fe_{0.12}Cr_{0.88}$, measured in a 100 Oe field. Circles: zero field cooling process. Squares: field cooling process.

ture. We study this phenomenon using two different measuring procedures: (i) In-field relaxation After a ZFC process from the paramagnetic regime to the measurement temperature, a field H is abruptly turned on and the slow response is recorded for 5 m. (ii) Isothermal remanent magnetization (IRM). The field of the previous procedure is turned off and the relaxation is measured for 5 m.

For both procedures the results have been fitted either to a power law

$$M = M_0 t^a \tag{1}$$

or to a logarithmic function

$$M = M_1 + S \ln t. \tag{2}$$

In all cases the exponent $a \ll 1$ and we are not able to distinguish between the two decay functions. Note, however, that in this limit ($a \ll 1$) we have

$$a = S/M \approx S/M_1. \tag{3}$$

In the following, we describe the temperature, field and sample dependence of the parameters in the above equations.

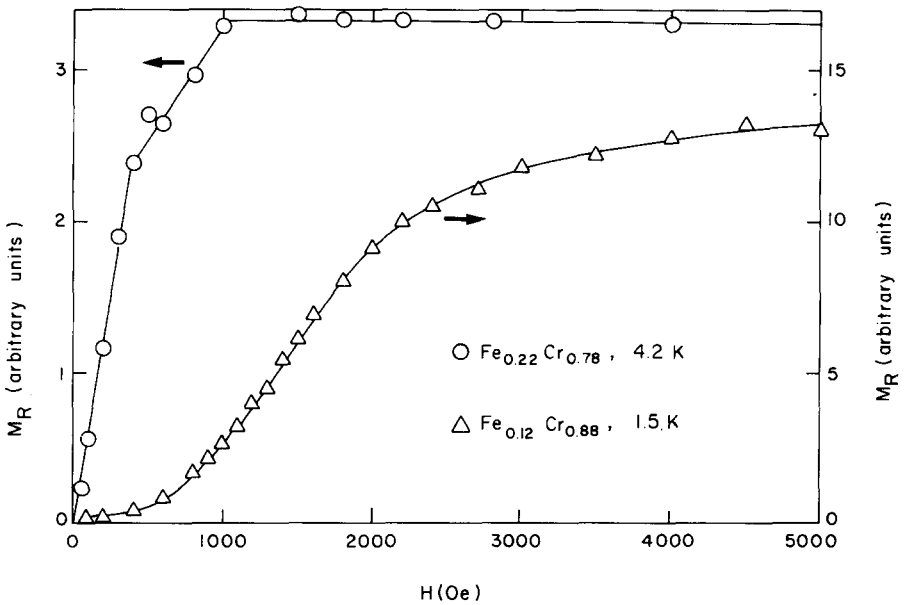

Fig. 3. Typical field dependence of the isothermal magnetic remanence, 2 min after turning off the field. Saturation values are 0.62 and 1.15 emu/g for the $x = 22$ and $x = 22$ samples, respectively.

3.1. Isothermal remanent magnetization

To study the field dependence of the IRM we describe in fig. 3 some typical results of $M_R(H)$ which were taken at a fixed time $t = 2$ min following the switching off of the field. As in many other spin glass systems [17] M_R increases with field and reaches a saturated value for a field H_S. The saturating field increases with decreasing temperature. The value of the remanence for fields $H \geq H_S$ seems to bear valuable information about the spin-glass phase borders. We chose a 5 kOe field ($H_S < 5$ kOe in *all* cases) for a study of the sample dependence of the remanence at different isotherms (fig. 4). The spin-glass $Fe_{0.16}Cr_{0.84}$ seems to have the highest M_R values. A change in the iron concentration in either direction causes a decrease in M. The nature of the isothermal solid curves in fig. 4 suggests a sharp, almost temperature independent cut-off of the spin glass phase at $x \approx 0.24$ whereas at the AFM side the SG border is pushed gradually to higher temperature as Fe concentration is increased.

3.2. In-field relaxation

The relaxation rate S, eq. (2), depends on field and temperature. A typical field dependence is shown in fig. 5. The field H_m for which $S(H)$ peaks increases with decreasing temperature. The rapid decrease of S with field changes gradually to a moderate slope until a zero value of S is found for a critical field $H_c(T)$. Extrapolation of S to a zero value is done [15] by fitting data points to $S \propto (1 - H/H_c)^{\nu}$. We find the exponent ν to vary between 1.5 and 2.5. The critical field $H_c(T)$ which is found via this procedure, is in good agreement with results obtained via the exponent a as will be described in a later paragraph.

Fig. 6 exhibits typical $S(T)$ curves. Here we define a critical temperature $T_c(H)$ above which viscosity phenomena vanish. It is seen clearly that T_c decrease with the increase of the magnetic field.

The field dependence of the exponent a is shown in fig. 7. Also here we find critical field $H_c(T)$, below which relaxation is still observed, by fitting data points to a power law $a \propto (1 - H/H_c)^{\phi}$, $\phi =$

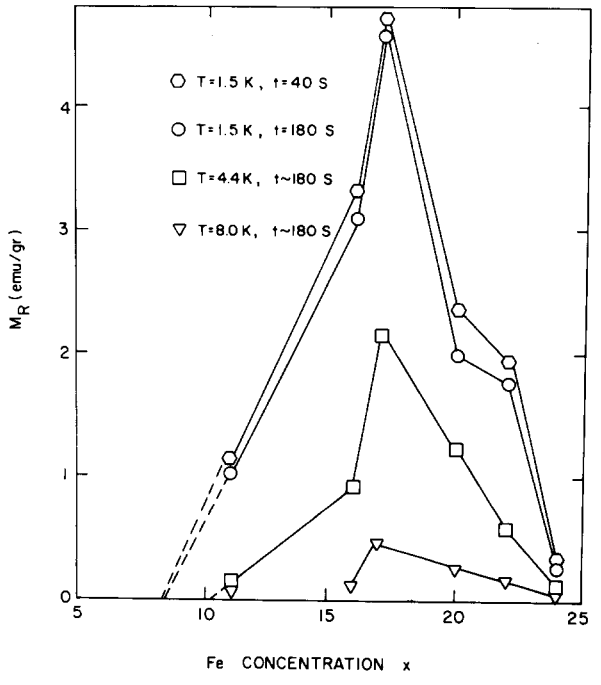

Fig. 4. Isothermal remanent magnetization for the various FeCr alloys.

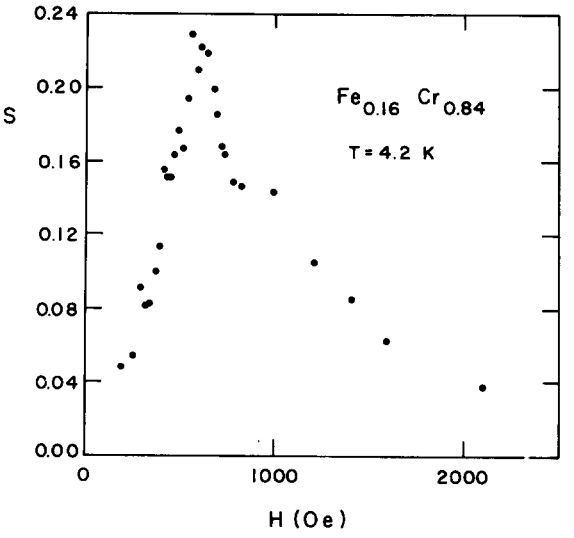

Fig. 5. Field dependence of the relaxation rate for $Fe_{0.16}Cr_{0.84}$ at $T = 4.2$ K.

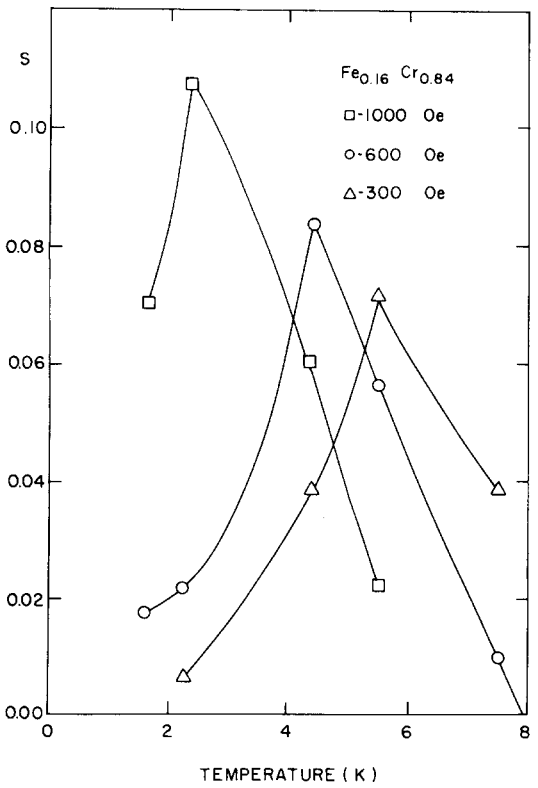

Fig. 6. Temperature dependence of the relaxation rate for $Fe_{0.16}Cr_{0.84}$.

2.4 ± 0.4. The extrapolation to zero viscosity introduces uncertainties in $H_c(T)$. This can be bypassed by using the scaling properties of this data [16]. (A similar approach was applied by Salamon and

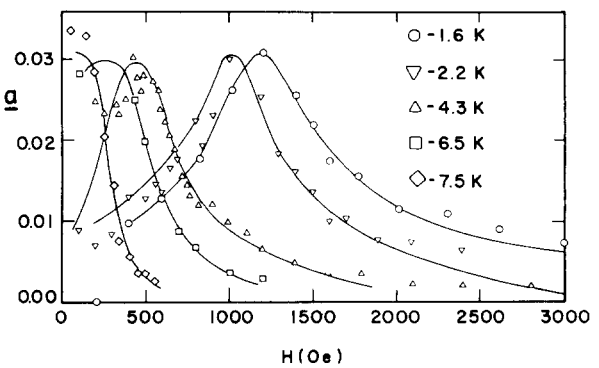

Fig. 7. Field dependence of the exponent a of eq. (1) for $Fe_{0.16}Cr_{0.84}$.

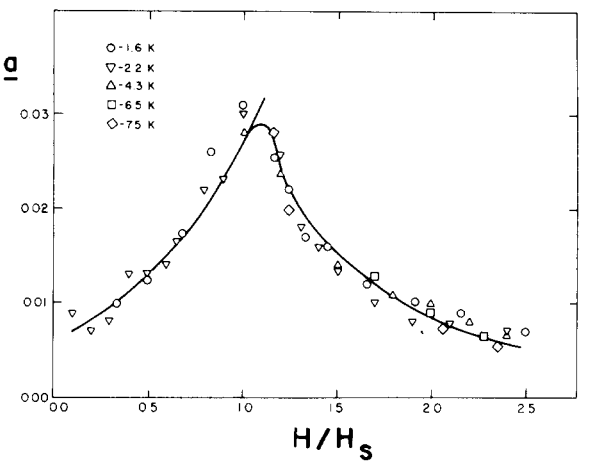

Fig. 8. Exponents $a(H)$ of fig. 7 scaled to a single curve by using a field parameter $H_S(T)$.

Tholence [15] to their $S(H, T)$ data.) We demonstrate it here in fig. 8 where $a(H)$ data points from five isotherms [16] are scaled with a field parameter H_s to give a "universal" $a(H/H_s)$ curve. The fields $H_s(T)$ are proportional to $H_c(T)$ and this gives quite an accurate determination, except for a proportionality factor, of the AT line. With the

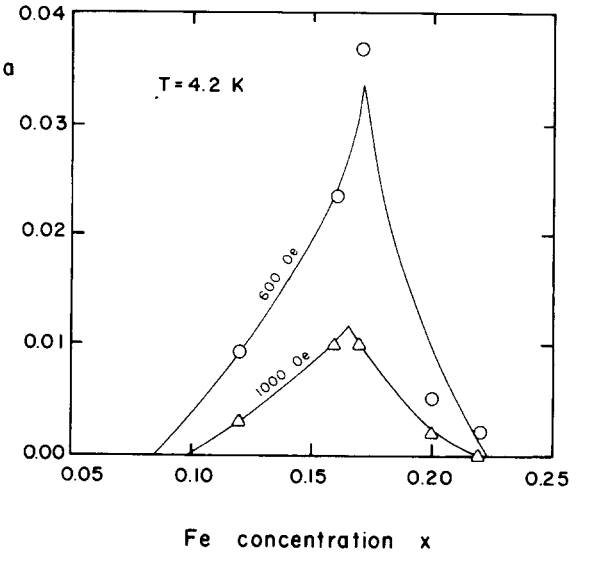

Fig. 9. Fe concentration dependence of the exponent a of eq. (1) for two different fields.

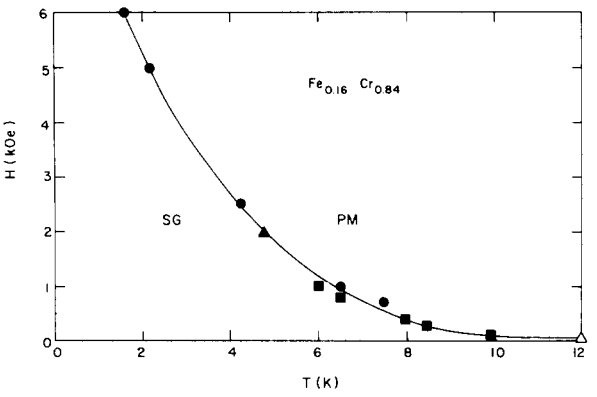

Fig. 10. Temperature-field phase diagram for $Fe_{0.16}Cr_{0.84}$.

proportionality factor, which is 5 ± 1, one obtains absolute values for the critical fields which are in good agreement with those obtained above, via analysis of $S(H)$ curves.

The iron-concentration dependence of the exponent is described in fig. 9 for 600 and 1000 Oe. This figure shows clearly the boundaries of the spin glass phase to different fields. Here, as in fig. 4, it seems that the border-line is much steeper at the FM side (around $x = 0.23$) than in the AFM side where a gradual change occurs in the spin glass regime due to external field.

In fig. 10 we summarize the $Fe_{0.16}Cr_{0.84}$ results in a temperature/field phase diagram. The circles describe points which are obtained via extrapolation of $a(H)$ curves to zero as discussed previously. The squares describe the result of similar extrapolation of $a(T)$ curves. The smooth solid line between experimental points approaches $T_f = 12.5$ K as $H_c = A(1 - T/T_f)^{\beta}$. We find $\beta = 2.3 \pm 0.4$ rather than 1.5 as predicted by mean field theory. Another serious deviation from theory occurs with regard to the proportionality factor A which is found to be smaller by more than an order of magnitude than the expected [9] value (which is of order 1). This indicates that the magnetic fields which are needed to induce the transition are much smaller than predicted theoretically. A similar trend was observed in other experiments [14–16,18,19], and reasons for this discrepancy have already been discussed [19,20]. Also, note that the lower field in fig. 10 is 100 Oe. Much lower fields might be needed for accurate determination of the AT line in this material.

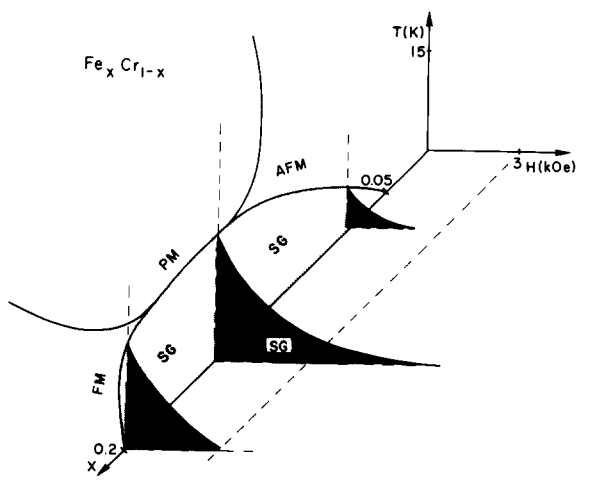

Fig. 11. Schematic $H-T-x$ phase diagram for FeCr.

Similar phase diagrams are obtained for the rest of the compositions under study. Qualitatively we find similar results but postpone quantitative considerations for a later publication. At this stage we may conclude that the spin glass phase in FeCr crystals is limited to a small range of compositions, temperature and magnetic field. In fig. 11 we summarize the present results in a schematic $H-T-x$ phase diagram.

We have found, in summary, that the application of a magnetic field to a spin glass leads to qualitative changes in the magnetic relaxation which is one of the main characteristics of the spin glass phase. We take the tendency of this relaxation to vanish above a critical field as evidence of a field induced SG/PM transitions as first suggested by de Almeida and Thouless. The theoretical predictions are still limited to "pure" $J_0 = 0$ spin glasses. The present results deal with a range of compositions which are certainly far from being "pure". Much more experimental *and* theoretical work remains to be done for a better understanding of the spin glass phase and the nature of the field induced transitions.

Acknowledgements

Thanks are due to H. Sompolinsky for discussing experimental implications of ref. [12] and to M.B. Salamon for sending us the results of ref. [15] prior to publication. Work in New York has been supported by the Office of Naval Research.

References

[1] S.F. Edwards and P.W. Anderson, J. Phys. F 5 (1975) 965.
[2] D. Sherrington and S. Kirkpatrick, Phys. Rev. Lett. 35 (1975) 1792.
[3] C.R. Fincher, S.M. Shapiro, A.C. Palumbo and R.D. Parks, Phys. Rev. Lett. 45 (1980) 474.
Y. Yeshurum, M.B. Salamon, K.V. Rao and H.S. Chen, Phys. Rev. Lett. 45 (1980) 1366.
[4] See, e.g., J. Dumas and C. Schlenker, J. Magn. Magn. Mat. 7 (1978) 252.
A. Berton, J. Chaussy, J. Odin, R. Rammal, J. Souletie, J.L. Tholence, R. Tournier, F. Holtzberg and S. Von Molnar, J. Appl. Phys. 52 (1981) 1763.
[5] S. Fishman and A. Aharony, Phys. Rev. B 21 (1980) 280.
[6] B. Babic, F. Kajzar and G. Parette, J. Phys. Chem. Solids 41 (1980) 1303, and references therein.
[7] V.E. Rode, S.A. Finkelberg, B. Wurl and A.I. Lyalin, Phys. Stat. Sol. (a) 64 (1981) 603.
[8] J.P. Strom-Olsen, D.F. Wilford, S.K. Burke and B.D. Rainford, J. Phys. F9 (1979) L95.
S.K. Burke and B.D. Rainford, J. Phys. F8 (1978) L239.
[9] J.R.L. de Almeida and D.J. Thouless, J. Phys. A 11 (1978) 983.
[10] G. Parisi, Phys. Rev. Lett. 23 (1979) 1754; J. Phys. A 13 (1980) 1887.
[11] M. Gabay and G. Toulouse, Phys. Rev. Lett. 47 (1981) 201.
[12] H. Sompolinsky, Phys. Rev. Lett. 47 (1981) 935.
[13] R.W. Knitter and J.S. Kouvel, J. Magn. Magn. Mat. 21 (1980) L316.
[14] Y. Yeshurun, L.J.P. Ketelsen and M.B. Salamon, Phys. Rev. B 26 (1982) 1491.
[15] M.B. Salamon and J.L. Tholence, Joint Intermag and MMM Conf., Montreal (1982).
J.L. Tholence and M.B. Salamon, J. Magn. Magn. Mat. 31–34 (1983) 1340.
M.B. Salamon and J.L. Tholence, J. Magn. Magn. Mat. 31–34 (1983) 1375.
[16] A.C. Palumbo, R.J. Parks and Y. Yeshurun, J. Phys. C 15 (1982) 837.
[17] See, e.g., H. v. Lohneysen and J.L. Tholence, Phys. Rev. B 19 (1979) 5858, and references therein.
[18] P. Monod and H. Bouchiat, J. Phys. Lett. 43 (1982) L45.
[19] Y. Yeshurun and H. Sompolinsky, Phys. Rev. B 26 (1982) 1487.
[20] R.V. Chamberlin, M. Hardiman, L.A. Turkevich and R. Orbach, Phys. Rev. B 25 (1982) 6720; these authors find a line whose field coefficient is of order 1.